

## Molecularly Imprinted Polymer Beads Prepared by Pickering Emulsion Polymerization for Steroid Recognition

Tongchang Zhou,<sup>1,2</sup> Xiantao Shen,<sup>1</sup> Shilpi Chaudhary,<sup>1,3,4</sup> Lei Ye<sup>1</sup>

<sup>1</sup>Division of Pure and Applied Biochemistry, Lund University, Box 124, 221 00 Lund, Sweden

<sup>2</sup>Guangzhou Pharmaceutical Holdings, Limited, Guangzhou 510130, China

<sup>3</sup>Division of Synchrotron Radiation Research, Lund University, Box 118, 22100 Lund, Sweden

<sup>4</sup>European Nano Invest, Fridhemsvägen 2, 217 74 Malmö, Sweden

Correspondence to: X. Shen (E-mail: xiantao.shen@tbiokem.lth.se) or L. Ye (E-mail: lei.ye@tbiokem.lth.se)

**ABSTRACT:** Pickering emulsion polymerization was used to synthesize molecularly imprinted polymer beads for the selective recognition of 17- $\beta$ -estradiol under aqueous conditions. Scanning electron microscopy analysis indicated that the imprinted polymer beads had a small diameter with a narrow size distribution ( $18.9 \pm 2.3 \mu\text{m}$ ). The reduction in particle size achieved in this study was attributed to the altered polarity of the stabilizing nanoparticles used in the Pickering emulsion. The imprinted polymer beads could be used directly in water and showed a high binding affinity for the template molecule, 17- $\beta$ -estradiol, and its structural analogs. These water-compatible polymer beads could be used as affinity adsorbents for the extraction and analysis of low-abundance steroid compounds in aqueous samples. © 2013 Wiley Periodicals, Inc. *J. Appl. Polym. Sci.* 000: 000–000, 2013

**KEYWORDS:** emulsion polymerization; molecular recognition; nanoparticles; nanowires and nanocrystals

Received 2 February 2013; accepted 1 June 2013; Published online

DOI: 10.1002/app.39606

### INTRODUCTION

Molecularly imprinted polymers (MIPs), as first reported by the groups of Wulff et al.<sup>1</sup> and Mosbach et al.,<sup>2</sup> are synthetic materials with a predesigned selectivity for a particular molecule of interest. Because of their low costs, higher stability, and easy preparation, MIPs have been used in affinity separation and various analytical applications.<sup>3</sup> Currently, MIPs are being used in several new fields, including optical sensors,<sup>4</sup> plastic antibodies,<sup>5</sup> and selective photocatalysis,<sup>6</sup> and to facilitate protein crystallization.<sup>7</sup> Mostly, MIPs are synthesized by the copolymerization of a functional monomer with an excess of crosslinking monomer in organic solvent.<sup>8</sup> The polymerization is carried out in the presence of a template molecule, which forms a supramolecular complex with the functional monomer to create an imprinted site. Although the simple molecular imprinting concept has led to numerous MIPs with high binding affinity and selectivity, the use of organic solvents brings in a disadvantage: poor binding selectivity in water due to the generally hydrophobic surface of MIPs. This problem has limited the application of MIPs in clinical and environmental analyses, where selective molecular binding is required under aqueous conditions.

Recently, several new methods have been developed to synthesize water-compatible MIPs.<sup>9–12</sup> Among these synthetic methods, we

exploited Pickering emulsion polymerization using a nanoparticle stabilizer in our previous studies to offer truly water-compatible MIPs.<sup>13,14</sup> In Pickering emulsion, fine solid particles are situated on the surface of emulsion droplets dispersed in an immiscible liquid; this thereby reduces the liquid–liquid surface tension and impedes the coalescence of the emulsion droplets. The unique three-phase structure of Pickering emulsion has been used to realize interesting functions in several applications, such as wastewater treatment and oil recovery.<sup>15–17</sup> As shown in the literature, Pickering emulsion has also been used to prepare new materials with more advanced structures.<sup>18</sup> When Pickering emulsion polymerization was used for molecular imprinting, it produced hydrophilic MIP beads that showed high molecular selectivity in water.<sup>19</sup> The hydrophilic surface and the molecular selectivity under aqueous conditions were attributed to the special polymerization conditions used: during the polymerization, the polar functional monomer, methacrylic acid (MAA), was enriched on the bead surface; this led to more carboxyl groups located on the bead surface. As a result, the MIP beads imprinted against the  $\beta$ -blocker, propranolol, showed a high molecular selectivity for the molecular template and its closely related molecular structures.

The aim of this study was to expand the scope of the Pickering emulsion polymerization method to synthesize different types of

Additional Supporting Information may be found in the online version of this article.

© 2013 Wiley Periodicals, Inc.

MIP beads. For this purpose, we selected 17- $\beta$ -estradiol as a model template because this steroid molecule has a very different polarity and functional groups in comparison with the previously used propranolol template. From the application point of view, this steroid template and many of its structural analogs have shown endocrine disrupting effects,<sup>20,21</sup> and their presence in environmental and drinking water needs to be carefully monitored.

In addition to retaining a favorable water compatibility, we also intended to decrease the size of the MIP beads to improve their binding kinetics; this is important for practical affinity separations using, for example, liquid chromatography. Because the nanoparticle stabilizer plays an important role in controlling the droplet size in Pickering emulsion, we used silica nanoparticles with a different polarity in this study to reduce the bead size of the MIPs from the previous 100–200 to 20  $\mu\text{m}$ . The MIP beads were characterized by fluorescence microscopy, SEM, and radioligand binding analysis to reveal their surface functional groups, particle size and morphology, and molecular recognition properties under aqueous conditions.

## EXPERIMENTAL

### Materials

SiO<sub>2</sub>-I (diameter = 10 nm, product number 637246) was purchased from Sigma-Aldrich (China). SiO<sub>2</sub>-II (diameter = 10 nm, product number 718483) and 17- $\beta$ -estradiol were purchased from Sigma (St. Louis, MO). Ethylene glycol dimethacrylate (EGDMA; 98%) was purchased from Sigma-Aldrich (Gillingham, United Kingdom). MAA (98.5%), 2,2-azobis(2-methylpropionitrile) (AIBN; 98%), and Triton X-100 (99.5%) were purchased from Merck (Darmstadt, Germany). Acriflavin (AFN; 90%) was supplied by Fluka (Dorset, United Kingdom). AIBN was recrystallized from methanol before use, and the other chemicals were analytical grade and were used as received. All of the aqueous solutions were prepared in ultrapure water (18 M $\Omega$  cm).

[2,4,6,7-<sup>3</sup>H(N)]-Estradiol (specific activity = 72.0 Ci/mmol, 13.9  $\mu\text{M}$  in ethanol), [1,2,6,7-<sup>3</sup>H(N)]-cortisol (specific activity = 60.0 Ci/mmol, 16.7  $\mu\text{M}$  in a 90:10 mixture of toluene and ethanol), L-[5-<sup>3</sup>H]-tryptophan (specific activity = 31 Ci/mmol, 32.3  $\mu\text{M}$  in a mixture of 50:50 water and ethanol), and [1,2,6,7-<sup>3</sup>H(N)]-corticosterone (specific activity = 82.0 Ci/mmol, 12.2  $\mu\text{M}$  in a 90:10 mixture of toluene and ethanol) were obtained from NEN Life Science Products, Inc. (Boston, MA). [1,2-<sup>3</sup>H(N)]-Cholesterol (specific activity = 41.3 Ci/mmol, 24.2  $\mu\text{M}$  in ethanol) and L-phenylalanine-[ring-2,6-<sup>3</sup>H(N)] (specific activity = 50.0 Ci/mmol, 20  $\mu\text{M}$  in a 98:2 mixture of water and ethanol) were obtained from Sigma. Before use, 10  $\mu\text{L}$  of the radioligands cortisol, L-tryptophan, and L-phenylalanine were dissolved in 10 mL of ethanol, and 10  $\mu\text{L}$  of the radioligands 17- $\beta$ -estradiol, corticosterone, and cholesterol were dissolved in 10 mL of acetonitrile. These stock solutions of radioligands were further diluted in the different solvents used in the radioligand binding analysis.

### Attenuated Total Reflection (ATR)–Fourier Transform Infrared (FTIR) Analysis

To investigate the surface properties of the silica nanoparticles, the dry particles were transferred onto the sample plate of the

**Table I.** Preparation of the MIP Beads by Pickering Emulsion Polymerization

Polymer	Template	Preheating time (h)	Liquid phase <sup>a</sup>
MIP1	17- $\beta$ -Estradiol	0	Water phase
MIP2	17- $\beta$ -Estradiol	0.5	Water phase
MIP3	17- $\beta$ -Estradiol	1	Water phase
MIP4	17- $\beta$ -Estradiol	0	Oil phase
MIP5	Corticosterone	0.5	Water phase

<sup>a</sup>The liquid phase to which the SiO<sub>2</sub>-II nanoparticles were first added.

FTIR instrument. ATR infrared spectra were recorded with a PerkinElmer FTIR instrument (PerkinElmer Instruments). All of the spectra were collected at room temperature in the range 4000–500  $\text{cm}^{-1}$  with 16 scans.

### $\zeta$ -Potential Measurement

The  $\zeta$  potential of the silica nanoparticles was measured by the laser Doppler electrophoresis technique with a Zetasizer Nano ZS instrument (Malvern Instruments, United Kingdom). Silica nanoparticles were suspended in ultrapure water at a concentration of 10  $\mu\text{g}/\text{mL}$  and introduced into folded capillary cells. The measurement was carried out at 25°C and repeated three times.

### Preparation of the Pickering Emulsion

SiO<sub>2</sub>-I (10 mg) or SiO<sub>2</sub>-II (10 mg), MAA (136  $\mu\text{L}$ ), NaOH solution (0.25 mL, 3 M), and Triton X-100 solution (3 mL, 0.3%) were mixed and sonicated for 10 min. After the addition of EGDMA (864  $\mu\text{L}$ ), toluene (100  $\mu\text{L}$ ), and AIBN (10 mg), the mixture was again sonicated for 10 min and shaken vigorously for about 1 min by hand.

### Preparation of the MIP Beads by Pickering Emulsion Polymerization

A stable Pickering emulsion contains three phases: solid particles, a water phase, and an oil phase. In this study, we used silica nanoparticles (SiO<sub>2</sub>-II, 10 mg) as the solid particles; a mixture of Triton X-100 solution (3 mL, 0.3%), NaOH solution (3M, 0.25 mL), and MAA (136  $\mu\text{L}$ ) as the water phase; and a mixture of EGDMA (864  $\mu\text{L}$ ), template (15 mg), and toluene (100  $\mu\text{L}$ ) as the oil phase. MIP beads were synthesized by Pickering emulsion polymerization under the conditions summarized in Table I.

Typically, SiO<sub>2</sub> nanoparticles and one liquid phase were mixed in a glass bottle and sonicated for 10 min. After the addition of the other liquid phase, the mixture was sonicated for 10 min and shaken vigorously for about 1 min by hand to give a stable Pickering emulsion. The Pickering emulsion was then prewarmed at 70°C for different periods (0, 0.5, and 1 h). Thereafter, 10 mg of AIBN was added to the prewarmed Pickering emulsion. The mixture was shaken vigorously for 1 min, heated to 70°C in an oven, and kept for 16 h without agitation. After the polymerization, the mixture was cooled to room temperature and kept there for 1 h to allow the polymer beads to settle before the supernatant was removed. The solid particles were washed with methanol two times, transferred into a plastic tube, and stirred in a mixture of 20 mL of methanol and 1 mL

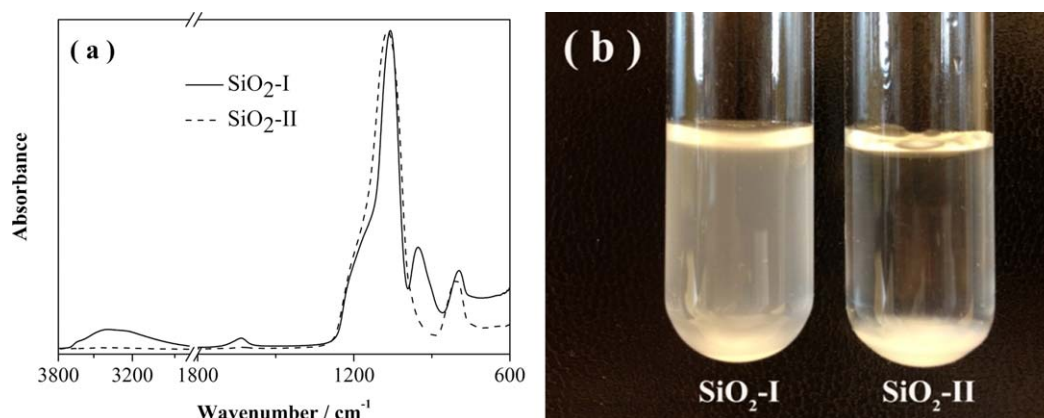


**Figure 1.** (a) FTIR spectra of the SiO<sub>2</sub>-I and SiO<sub>2</sub>-II nanoparticles. (b) Images of the SiO<sub>2</sub>-I and SiO<sub>2</sub>-II nanoparticles dispersed in water. [Color figure can be viewed in the online issue, which is available at [wileyonlinelibrary.com](http://wileyonlinelibrary.com).]

of HF (30%) at room temperature for 12 h to remove the silica nanoparticles. To remove the template, the solid polymer microspheres were washed with methanol containing 10% acetic acid until no template could be detected in the washing solvent. Finally, the polymer particles were washed with acetone and dried in a vacuum chamber. As a control, nonimprinted polymer (NIP) microspheres were prepared in the same way, except that no template was added.

#### Morphology of the Pickering Emulsion

The Pickering emulsions were dropped onto a glass slide and observed with a Nikon Eclipse E400 epifluorescence microscope equipped with a charge-coupled device camera.

#### Surface Characterization of the MIP Beads

A scanning electron microscope (Thermal Field Emission SEM LEO 1560, Zeiss, Oberkochen, Germany) was used to observe the surface morphology of the MIP beads.

#### Fluorescent Labeling with AFN

The carboxyl groups on the MIP or NIP particles were labeled with a fluorescent dye, AFN.<sup>22</sup> Briefly, 5 mg of particles was added to 1 mL of AFN solution (100 mg/L in methanol), and the mixture was stirred at room temperature in the dark for 16 h. The particles were separated by centrifugation and washed with methanol until no fluorescence could be observed in the supernatant. The particles were finally dried in a vacuum chamber. The AFN-labeled microspheres were deposited on a glass slide and observed with the Nikon Eclipse E400 epifluorescence microscope equipped with a charge-coupled device camera.

#### Radioligand Binding Analysis

MIP beads (5 mg) were added to 1 mL of solvent. After the addition of 20  $\mu$ L of a stock solution of radioligand {containing [2,4,6,7-<sup>3</sup>H]-estradiol (278 fmol), [1,2,6,7-<sup>3</sup>H(N)]-cortisol (334 fmol), [1,2,6,7-<sup>3</sup>H(N)]-corticosterone (244 fmol), L-phenylalanine-[ring-2,6-<sup>3</sup>H(N)] (400 fmol), [1,2-<sup>3</sup>H(N)]cholesterol (484 fmol), or L-[5-<sup>3</sup>H] tryptophan (646 fmol)}, the mixture was stirred gently at room temperature for 16 h. After centrifugation, 500  $\mu$ L of supernatant was collected and added to 10 mL of scintillation liquid (Ecoscint A), and the radioactivity was measured with a Tri-Carb 2800TR liquid scintillation analyzer

(PerkinElmer). The difference between the free radioligand and the total radioligand added was used to calculate the percentage of binding.

## RESULTS AND DISCUSSION

In recent years, MIPs for 17- $\beta$ -estradiol have been prepared with different synthetic methods.<sup>23–25</sup> However, most of these MIPs showed molecular recognition capability only in organic solvents. Although in some studies traditional MIPs have been tested in water, the specific binding in water displayed by these MIPs has generally been very low. Therefore, it is necessary to study new approaches to synthesize MIPs that can selectively recognize 17- $\beta$ -estradiol, particularly under aqueous conditions. In our previous study, we showed that MIP beads synthesized by Pickering emulsion polymerization displayed favorable molecular recognition for propranolol and its structural analogs in water. The excellent water compatibility was explained to be a result of the hydrophilic surface of the MIP beads, which was created by the special partition of the polar functional monomer MAA on the oil–water interface during the polymerization. To investigate whether the Pickering emulsion polymerization method could be applied to other template systems, we synthesized 17- $\beta$ -estradiol-imprinted polymer beads and characterized the molecular recognition properties of the obtained MIP beads. In addition to preparing new water-compatible MIP beads, we also studied how to reduce the particle size of MIP beads by employing different types of nanoparticle stabilizers.

#### Control of the Droplet Size in Pickering Emulsions with Different SiO<sub>2</sub> Nanoparticles

The first aim of this study was to generate small MIP beads by Pickering emulsion polymerization. To test the applicability of Pickering emulsion polymerization, we kept the composition of the water and oil phase identical to that used in our previous study;<sup>19</sup> we only changed the nanoparticle stabilizer to control the size of the Pickering emulsion. Two types of SiO<sub>2</sub> nanoparticles with different polarities were selected to prepare the Pickering emulsion. The surface properties of the silica nanoparticles were first studied by ATR–FTIR analysis. As shown in Figure 1(a), the broad peak around 3400  $\text{cm}^{-1}$ , the

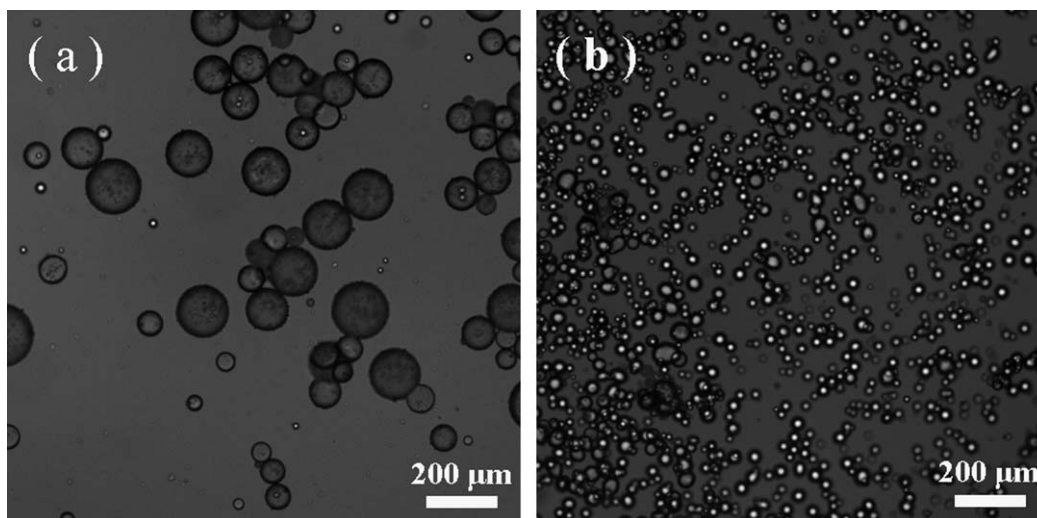


**Figure 2.** Optical images of the Pickering emulsion from the (a) SiO<sub>2</sub>-I and (b) SiO<sub>2</sub>-II nanoparticles.

sharp peak at 1629 cm<sup>-1</sup>, and the peak at 953 cm<sup>-1</sup> were assigned to the fundamental stretching vibrations of O—H group, the bending vibrations of coordinated Si—OH, and the in-plane stretching vibrations of Si—OH group, respectively.<sup>26,27</sup> For clearer comparison, the IR spectra were normalized to give the same intensity for the asymmetric Si—O—Si stretching vibration peaks around 1100 cm<sup>-1</sup>.<sup>27</sup> Apparently, the density of OH groups on SiO<sub>2</sub>-I was much higher than that on SiO<sub>2</sub>-II; this suggested that SiO<sub>2</sub>-I was more hydrophilic than SiO<sub>2</sub>-II. The different surface polarities between SiO<sub>2</sub>-I and SiO<sub>2</sub>-II were also confirmed by the measurement of their colloidal stability in water. When 10 mg of the different SiO<sub>2</sub> nanoparticles were added to 3 mL of water, SiO<sub>2</sub>-I produced a more stable dispersion than SiO<sub>2</sub>-II, which aggregated and settled quickly [Figure 1(b)]. The different hydrophilicities and colloidal stabilities of SiO<sub>2</sub>-I and SiO<sub>2</sub>-II in water were further confirmed by the measurement of their  $\zeta$  potentials. For the nanoparticles suspended in ultrapure water, the  $\zeta$  potentials of SiO<sub>2</sub>-I and SiO<sub>2</sub>-II were

found to be -36.5 and -33.6 mV, respectively. The more negative  $\zeta$  potential of SiO<sub>2</sub>-I also supported the fact that SiO<sub>2</sub>-I was more hydrophilic than SiO<sub>2</sub>-II; this led to the higher colloidal stability of SiO<sub>2</sub>-I in water [Figure 1(b)].

In comparison with an emulsion stabilized by surfactant, the mechanism of Pickering emulsion appears to be more complicated. One important factor is that the surface characteristics of SiO<sub>2</sub> particles affect the morphology and droplet size of the obtained Pickering emulsions. Figure 2 shows the microscope images of the Pickering emulsions stabilized by SiO<sub>2</sub>-I and SiO<sub>2</sub>-II. The emulsions stabilized by SiO<sub>2</sub>-I had a wide size distribution from 20 to 200  $\mu$ m. When SiO<sub>2</sub>-II nanoparticles were used as the stabilizer to prepare the Pickering emulsions, the dispersed droplets became much smaller ( $\sim$ 20  $\mu$ m). The reduced droplet size in the Pickering emulsion should have led to MIP beads with similar diameters after the imprinting reaction, and these MIP beads should be more suitable as stationary

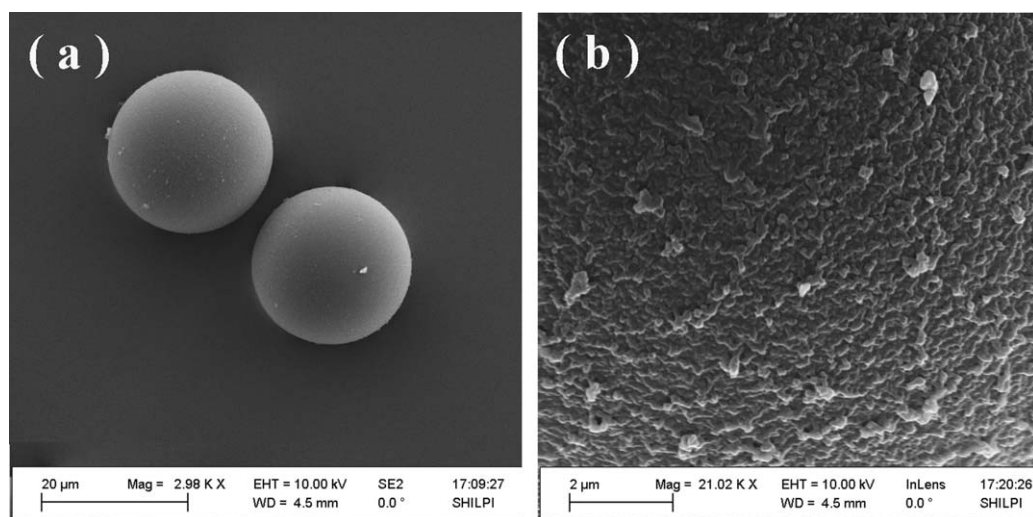


**Figure 3.** SEM images of the (a) MIP2 beads and (b) their surface morphology after the silica nanoparticles were removed.

**Table II.** Radioligand Binding Analysis for the Polymers in Different Solvents

Solvent	Uptake of the 17- $\beta$ -estradiol (%)									
	MIP1	NIP1	SU <sup>b</sup>	MIP2	NIP2	SU	MIP3	NIP3	MIP4	SU
Water	59.0 $\pm$ 2.1	36.6 $\pm$ 1.8	22.4	55.2 $\pm$ 2.3	26.4 $\pm$ 1.5	28.8	45.1 $\pm$ 2.5	13.9 $\pm$ 1.3	63.2 $\pm$ 2.6	31.2
Buffer <sup>a</sup>	45.4 $\pm$ 2.9	28.4 $\pm$ 0.9	17.0	45.1 $\pm$ 4.3	18.9 $\pm$ 1.1	26.2	22.6 $\pm$ 2.1	4.6 $\pm$ 0.9	57.0 $\pm$ 3.1	18.0
Toluene	10.0 $\pm$ 0.6	9.5 $\pm$ 0.4	0.5	9.5 $\pm$ 1.8	5.6 $\pm$ 0.4	3.9	6.7 $\pm$ 0.9	5.4 $\pm$ 0.5	12.0 $\pm$ 1.9	1.3
Acetonitrile	5.2 $\pm$ 3.7	7.1 $\pm$ 0.9	-1.9	5.9 $\pm$ 2.0	4.5 $\pm$ 1.3	1.4	1.1 $\pm$ 0.7	0.7 $\pm$ 0.3	3.3 $\pm$ 3.1	0.4

<sup>a</sup> Tris buffer, pH 8.2.

<sup>b</sup> SU, specific uptake, which was defined as the difference in the estradiol uptake between the MIP and NIP.

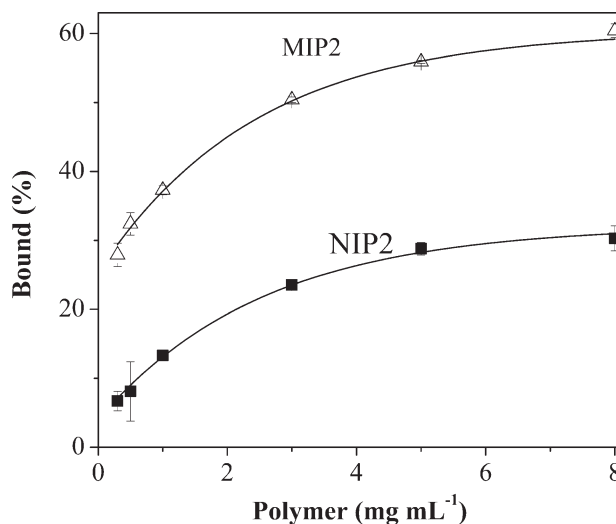


**Figure 4.** Uptake of 17- $\beta$ -estradiol by different amounts of MIP2 and NIP2.

phases in chromatography separations.<sup>28</sup> In the remaining experiments, we focused on preparing MIP beads with Pickering emulsion stabilized by SiO<sub>2</sub>-II nanoparticles.

#### Characterization of the MIP Beads: Fluorescence Microscopy and SEM Analysis

Because of the solubility of the functional monomer MAA in both the water and oil phases, the MIP beads obtained by Pickering emulsion polymerization tended to have abundant carboxyl groups on their surface.<sup>14</sup> To investigate the functional groups on the surface of this 17- $\beta$ -estradiol imprinted MIP and the control polymer (NIP), the two polymers were labeled with AFN and then inspected with a fluorescence microscope. In Figure S1 (see the Supporting Information), the two labeled polymers showed strong fluorescence emission; this indicated the presence of a high density of carboxyl groups on the surface of the particles. From the fluorescence microscope images, the sizes of the MIP and NIP beads were calculated to be

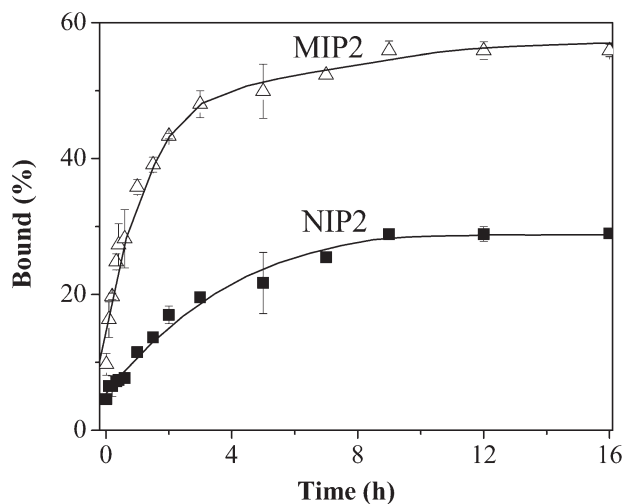


**Figure 5.** Kinetic adsorption curves for the 17- $\beta$ -estradiol binding on MIP2 and NIP2.

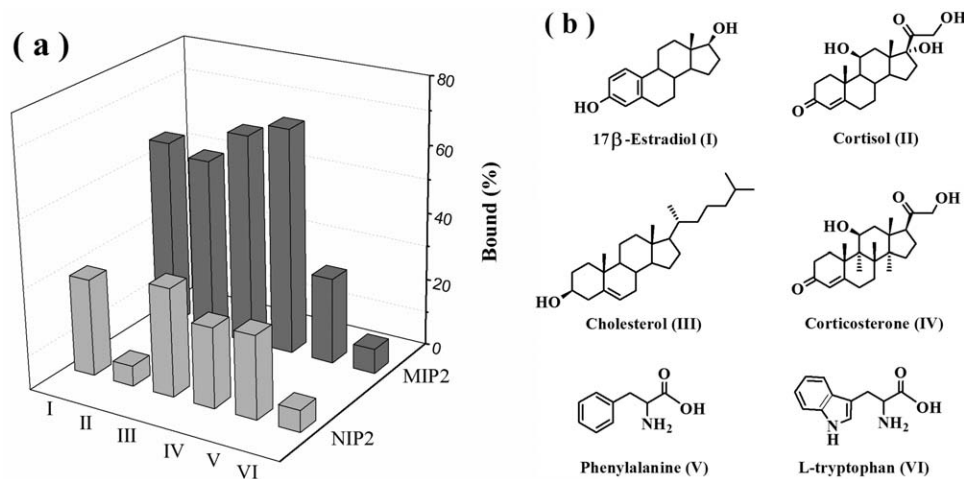


**Figure 6.** (a) Uptake of the test compounds by MIP2 and NIP2 in water. (b) The structures of the test analytes.

$18.9 \pm 2.3$  and  $18.2 \pm 2.7$   $\mu\text{m}$ , respectively. Therefore, the size of these polymer beads indeed followed the droplet size of the respective Pickering emulsions stabilized by  $\text{SiO}_2$ -II nanoparticles [Figure 2(b)].

In Pickering emulsions, silica particles are self-assembled at the oil/water interface. After polymerization and the removal of the silica particles, open pores were left on the surface of the imprinted beads. In Figure 3(a), the SEM image showed clearly the spherical shape of the MIP beads. The image in Figure 3(b) revealed the rough surface of the same polymer after the silica nanoparticles were removed.

#### Molecular Binding Characteristics of the MIP Beads

To study the molecular recognition properties of the synthesized MIP beads, we first carried out a radioligand binding experiment under equilibrium conditions.<sup>29</sup> The uptake of 17- $\beta$ -estradiol in different solvents is summarized in Table II. When tested in toluene, all of the MIP beads showed a higher specific binding than in acetonitrile; this could be explained by the more favorable H-bond interactions between the template and the imprinted sites in the less polar solvent. The radioligand binding results presented in Table II suggest that the MIP beads displayed the highest specific binding for 17- $\beta$ -estradiol in aqueous solvent. This feature was similar to that of the previously reported MIP beads prepared by Pickering emulsion polymerization with propranolol as template.<sup>19</sup> The specific 17- $\beta$ -estradiol binding in water could be explained by the existence of carboxyl groups on the surface of the MIP beads. The increased hydrophilicity of the MIP beads should have contributed to a reduction in the nonspecific binding, as indicated by the adsorption on the NIP beads. As both the MIP and the NIP beads had lower 17- $\beta$ -estradiol binding in toluene and acetonitrile, the specific binding in water seemed to have been driven mainly by hydrophobic interactions. Despite the polar surfaces of the MIP beads, it is possible that within the molecularly imprinted cavities, the well-defined hydrophobic sites played an important role in the specific binding.

From Table II, it is also shown that the order of mixing in the water and oil phases during the preparation of the Pickering

emulsions did not affect the nonspecific binding in water (see NIP1 and NIP4). Also, the mixture of the silica nanoparticles first with the oil phase before they were added to the water phase only led to a slightly increased specific binding (for MIP4). Interestingly, the nonspecific binding of the MIP beads decreased significantly when the emulsions were prewarmed at 70°C before the polymerization was initiated (see MIP1, MIP2, and MIP3). The preheating may have increased the molecular complexation driven by hydrophobic interactions; this thereby led to better imprinted cavities. As a higher specific binding in both water and buffer was observed in the MIP2/NIP2 system, in the remaining experiments we focused on studying these two polymers in more detail.

Figure 4 shows the increased uptake of estradiol when more polymer beads (MIP2 and NIP2) were added. For both MIP2 and NIP2, increasing the amount of polymer increased the uptake of 17- $\beta$ -estradiol, but because of the molecular imprinting effect, MIP2 always showed a higher binding for 17- $\beta$ -estradiol (2–4 times) than NIP2. To investigate the kinetics of binding, we measured the uptake of the radioligand after the polymer beads were incubated with the radioligand for different periods. From the kinetic adsorption curves shown in Figure 5, it was clear that the time required to reach equilibrium binding was about 9 h for both MIP2 and NIP2. The MIP beads synthesized in this study had much slower binding kinetics than our previously reported surface-imprinted particles, which could reach binding equilibrium in 20 min.<sup>14</sup> Nevertheless, the presence of more abundant imprinted sites over the whole particle volume resulted in a much improved binding capacity. Further improvement to increase binding kinetics may be achieved by optimization of the type and quantity of the porogenic solvent used in the Pickering emulsion polymerization.

The selectivity of the 17- $\beta$ -estradiol-imprinted polymer (MIP2) was studied by the measurement of its uptake of other steroid compounds (cortisol, cholesterol, and corticosterone) and two unrelated structures (phenylalanine and L-tryptophan) at similar low concentrations. To focus on studying the best imprinted sites, we decided to perform all of the equilibrium binding using radioligands in the same concentration range (244–646 pM).

The uptake of these compounds by MIP2 and NIP2 in water is depicted in Figure 6, where the structures of these analytes are also shown. It was interesting to observe that the binding of 17- $\beta$ -estradiol (I), cortisol (II), cholesterol (III), and corticosterone (IV) followed a similar pattern (i.e., the uptake of these radioligands by MIP2 was significantly higher than that by NIP2), and MIP2 showed a general selectivity for the steroid structures. For the non-related phenylalanine and L-tryptophan, MIP2 did not show any increased binding compared to NIP2. The preference of MIP2 to selectively bind the similar steroid structures was attributed to the presence of the 17- $\beta$ -estradiol-imprinted sites, which could also accommodate cortisol, cholesterol, and corticosterone under the same aqueous conditions. It was interesting to note that when corticosterone was used as the template, the imprinted polymer synthesized under the same conditions (MIP5) only showed marginal specific binding for corticosterone (see Figure S2 in the Supporting Information). Therefore, the group selectivity displayed by MIP2 was, in fact, useful for analytical separation of some steroids that are known to give poor molecular imprinting effects.<sup>30</sup>

## CONCLUSIONS

In this study, MIP beads that were water-compatible toward 17- $\beta$ -estradiol were prepared by Pickering emulsion polymerization. Instead of the previously used hydrophilic silica, more hydrophobic silica nanoparticles were used to prepare the Pickering emulsion with smaller droplet sizes; this reduced the size of the MIP beads from about 150 to about 20  $\mu\text{m}$ . Under optimized conditions, the synthesized MIP beads showed a high affinity for 17- $\beta$ -estradiol and similar steroid structures in aqueous solvent. The specific binding for the similar steroid structures was attributed to the combined hydrophobic and hydrogen-bond interactions located in the imprinted cavities. We expect that the group selectivity of this 17- $\beta$ -estradiol imprinted beads should enable the direct extraction of steroid compounds and other endocrine disrupting chemicals from environmental water. Research in this direction is ongoing and will be reported in a future publication.

## ACKNOWLEDGMENTS

This work was supported by the Swedish Research Council for Environment, Agricultural Sciences and Spatial Planning (FORMAS).

## REFERENCES

1. Wulff, G.; Sarhan, A.; Zabrocki, K. *Tetrahedron Lett.* **1973**, *44*, 4329.
2. Vlatkis, G.; Andersson, L. I.; Muller, R.; Mosbach, K. *Nature* **1993**, *361*, 645.
3. Jiang, M.; Shi, Y.; Zhang, R.; Shi, C.; Peng, Y.; Huang, Z.; Lu, B. *J. Sep. Sci.* **2009**, *32*, 3265.
4. Salma, A.-K.; Rosana, B.; Luis, S. R. J.; Elena, D. G. M. *Crit. Rev. Anal. Chem.* **2000**, *30*, 291.
5. Hoshino, Y.; Kodama, T.; Okahata, Y.; Shea, K. J. *J. Am. Chem. Soc.* **2008**, *130*, 15242.
6. Shen, X.; Zhu, L.; Wang, N.; Ye, L.; Tang, H. *Chem. Commun.* **2012**, *48*, 788.
7. Saridakisa, E.; Khurshidb, S.; Govadab, L.; Phanc, Q.; Hawkinsc, D.; Crichlowd, G. V.; Lolisd, E.; Reddyc, S. M.; Chayenb, N. E. *Proc. Natl. Acad. Sci.* **2011**, *108*, 11081.
8. Ansell, R. J.; Mosbach, K. *J. Chromatogr. A* **1997**, *787*, 55.
9. Dirion, B.; Cobb, Z.; Schillinger, E.; Andersson, L. I.; Sellergren, B. *J. Am. Chem. Soc.* **2003**, *125*, 15101.
10. Tatemichi, M.; Sakamoto, M.; Mizuhata, M.; Deki, S.; Takeuchi, T. *J. Am. Chem. Soc.* **2007**, *129*, 10906.
11. Puoci, F.; Lemma, F.; Cirillo, G.; Curcio, M.; Parisi, O. I.; Spizzirri, U. G.; Picci, N. *Eur. Polym. J.* **2009**, *45*, 1634.
12. Ma, Y.; Zhang, Y.; Zhao, M.; Guo, X.; Zhang, H. *Chem. Commun.* **2012**, *48*, 6217.
13. Shen, X.; Ye, L. *Chem. Commun.* **2011**, *47*, 10359.
14. Shen, X.; Ye, L. *Macromolecules* **2011**, *44*, 5631.
15. Dinsmore, A. D.; Hsu, M. F.; Nikolaidis, M. G.; Marquez, M.; Bausch, A. R.; Weitz, D. A. *Science* **2002**, *298*, 1006.
16. Colver, P. J.; Colard, C. A. L.; Bon, S. A. F. *J. Am. Chem. Soc.* **2008**, *130*, 16850.
17. Thompson, K. L.; Armes, S. P.; Howse, J. R.; Ebbens, S.; Ahmad, I.; Zaidi, J. H.; York, D. W.; Burdis, J. A. *Macromolecules* **2010**, *43*, 10466.
18. Binks, P. *Adv. Mater.* **2002**, *14*, 1824.
19. Shen, X.; Xu, C.; Ye, L. *Soft Matter* **2012**, *27*, 3169.
20. Wang, S.; Huang, W.; Fang, G.; Zhang, Y.; Qiao, H. *J. Environ. Anal. Chem.* **2008**, *88*, 1.
21. Kimura, A.; Taguchi, M.; Arai, H.; Hiratsuka, H.; Namba, H.; Kojima, T. *Radiat. Phys. Chem.* **2004**, *69*, 295.
22. Ivanov, V. B.; Behnisch, J.; Hollander, A.; Mehdorn, F.; Zimmermann, H. *Surf. Interface Anal.* **1996**, *24*, 257.
23. Rachkov, A.; McNiven, S.; El'skayab, A.; Yanoa, K.; Karube, I. *Anal. Chim. Acta* **2000**, *405*, 23.
24. Ye, L.; Cormack, P. A. G.; Mosbach, K. *Anal. Chim. Acta* **2001**, *435*, 187.
25. Celiz, M. D.; Aga, D. S.; Colon, L. A. *Microchem. J.* **2009**, *92*, 174.
26. Shen, X.; Zhu, L.; Huang, C.; Tang, H.; Yu, Z.; Deng, F. *J. Mater. Chem.* **2009**, *19*, 4843.
27. Khalil, K. M. S.; Elsamahy, A. A.; Elanany, M. S. *J. Colloid Interface Sci.* **2002**, *249*, 359.
28. Lai, J.-P.; Lu, X.-Y.; Lu, C.-Y.; Ju, H.-F.; He, X.-W. *Anal. Chim. Acta* **2001**, *442*, 105.
29. Bui, B. T. S.; Belmont, A.-S.; Witters, H.; Haupt, K. *Anal. Bioanal. Chem.* **2008**, *390*, 2081.
30. Long, Y.; Philip, J. Y. N.; Schillén, K.; Liu, F.; Ye, L. *J. Mol. Recognit.* **2011**, *24*, 619.